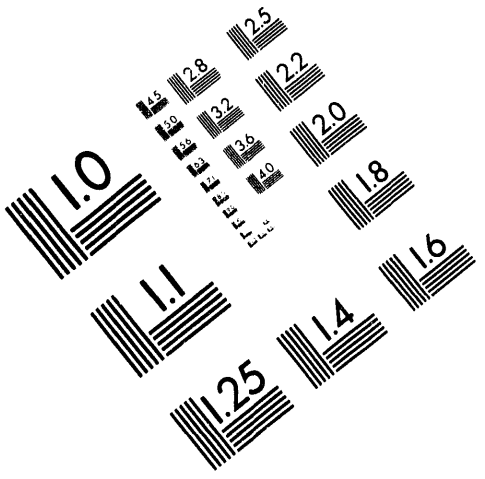

Association for Information and Image Management

1100 Wayne Avenue, Suite 1100
Silver Spring, Maryland 20910

301/587-8202

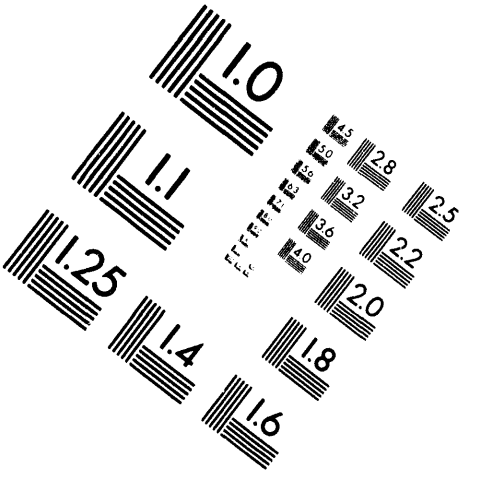

Centimeter

Inches

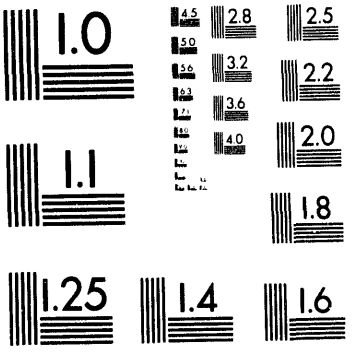

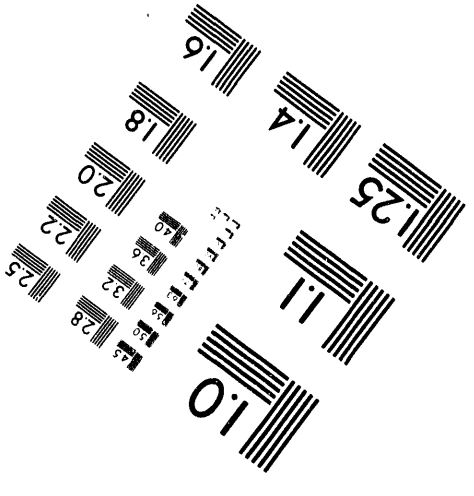

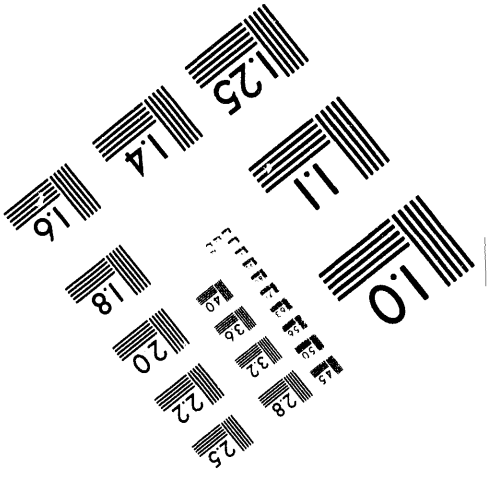

MANUFACTURED TO AIIM STANDARDS
BY APPLIED IMAGE, INC.

1 of 1

Investigation of Magnetic Reconnection during a Sawtooth Crash in a High Temperature Tokamak

by

M. Yamada, F. Levinton*, N. Pomphrey, R. Budney,
J. Macickam and Y. Nagayama**

Princeton Plasma Physics Laboratory, Princeton University
P.O.Box 451, Princeton, New Jersey 08543

Abstract

This paper reports on a recent laboratory investigation on magnetic reconnection in high temperature tokamak plasmas. The motional stark effect(MSE) diagnostic is employed to measure the pitch angle of magnetic field lines, and hence the q profile. An analytical expression that relates pitch angle to q profile has been developed for a toroidal plasma with circular cross section. During the crash phase of sawtooth oscillations in the plasma discharges, the ECE (electron cyclotron emission) diagnostic measures a fast flattening of the 2-D electron temperature profile in a poloidal plane, an observation consistent with the Kadomtsev reconnection theory. On the other hand motional the MSE measurements indicate that central q values do not relax to unity after the crash, but increase only by 5-10%, typically from 0.7 to 0.75. The latter result is in contradiction with the models of Kadomtsev and/or Wesson. The present study addresses this puzzle by a simultaneous analysis of electron temperature and q profile evolutions. Based on a heuristic model for the magnetic reconnection during the sawtooth crash, the small change of q, i.e. partial reconnection, is attributed to the precipitous drop of pressure gradients which drive the instability and the reconnection process as well as flux conserving plasma dynamics.

---

*Fusion Physics and Technology Torrance, CA 90503
**University of Tsukuba, Japan

MASTER

I. Introduction

Magnetic reconnection, involves the breaking and topological rearrangement of magnetic field lines, and is an important relaxation process in plasma physics.[2–7] Sawtooth oscillations[8] in high temperature fusion plasmas are a manifestation of magnetic reconnection, and play an important role in determining confinement characteristics.[9–11] Magnetic reconnection is also a key process in the description of evolution mechanisms for solar flares,[3] the earth's magnetosphere[4] and some low temperature laboratory experiments.[5–7]

A sawtooth oscillation is characterized by a periodic collapse or crash of the central plasma pressure.[8–11] Although there are several theoretical models for the sawtooth, Kadomtsev's model[10] developed twenty years ago has attained the widest acceptance. According to this model an $m = n = 1$ resistive internal mode is unstable for $q_0 < 1$ (m and n are the poloidal and toroidal mode numbers and q_0 is the safety factor at the magnetic axis), and grows until a full magnetic reconnection process flattens the pressure and current profiles causing the central q value to increase to unity.

Evolution of the central q values have been measured by a number of groups for the past several years.[12–17] There is agreement among all experiments that the relative change of the central q during a sawtooth crash is small($\Delta q/q < 0.1$). However, there is a major difference among reported final values of the central q after the crash. Most recently, Wroblewski and Snider[17] reported that central q values on DIII-D[1] rise to unity, claiming that their observation is evidence of Kadomtsev reconnection.

The primary subject of the present paper is an experimental study of magnetic reconnection in high temperature TFTR(Tokamak Fusion Test Reactor)[1] plasmas (where the Magnetic Reynolds number exceeds 10^7) by a set of non-perturbative diagnostics. During the crash phase of sawtooth oscillations, ECE (electron cyclotron emission) and Soft-Xray diagnostic systems[18–20] observe that the temperature gradient inside the inversion radius diminishes to nearly zero after the crash. This observation is consistent with predictions of the Kadomtsev[10] model. However, $q(R)$ profiles measured by motional Stark effect (MSE) diagnostics[21] indicate that central q values increase typically from 0.7 to 0.8 during the sawtooth crash phase and do not relax to unity even while the pressure gradient diminishes inside the $q = 1$ region. This latter observation is an important contradiction with the theories of Kadomtsev[10] and Wesson.[11]

We address this puzzle by a simultaneous analysis of electron temperature and q profile evolution during sawtooth oscillations. Small changes of $q(R)$ are documented. Based on a heuristic model for magnetic reconnection during the sawtooth crash, the small change of q (implying limited reconnection) is attributed to the combined effects of flux conserving plasma dynamics and to the precipitous drop of the pressure

gradients which drive the instability and reconnection process.

II. Electron Temperature Evolution in Sawtooth Crash

The electron temperature profile on the midplane of the plasma is measured with a 20 channel grating polychrometer[21,18,19] and with a 2μsec time step covering $R = 2.1 - 3.4$m with a spatial channel separation of 6cm. A two-dimensional(2-D) electron temperature profile on a poloidal plane can be obtained by making use of the fast toroidal rotation of the plasma. The image reconstruction techniques using rotation have been described in a previous publication together with an analysis of the reconstruction errors.[18–20] The present work extends this 2-D imaging technique to elucidate electron heat flow during sawtooth oscillation.

Profiles of electron temperature in a poloidal plane, $T_e(r,\theta)$, are conveniently represented as three-dimensional(3-D) plots with the vertical axis denoting electron temperature. Changes in temperature profile during a sawtooth cycle can be represented by the differences $\Delta T_e(r,\theta,t) = T_e(r,\theta,t) - T_e^{base}(r,\theta)$, where $T_e^{base}(r,\theta)$ is a base profile equal to the lowest value of $T_e(r,\theta,t)$ obtained at location r,θ at any time during a given sawtooth cycle. Overlaying color contours of ΔT_e on the 3-D $T_e(r,\theta)$ profiles allows one to visualize[20] the inventory of electron thermal energy during a sawtooth period.

Fig. 1 shows the electron temperature profile evolution during a typical sawtooth crash, with overlayed color contours of ΔT_e depicting the transfer of electron thermal energy. The time interval between each of the four frames in the figure is $\approx 120\mu$sec, approximately equal to the plasma's toroidal rotation period at the time of the sawtooth crash. Fig. 1(a) shows an essentially axisymmetric pattern for T_e, giving no indication of the dramatic profile evolution that takes place between Fig. 1(b) and (c) during the sawtooth crash. Just before the collapse of the peak temperature, when the pressure reaches a threshold value, the temperature peak shifts radially within the inversion radius $r(q = 1)$ and shrinks in size. Also within the inversion radius is seen a growing crescent-shaped flat temperature region[22,23] corresponding to the development of a helical $m/n = 1/1$ kink mode. The T_e profile inside the inversion radius is nearly flat after the crash (see Fig. 1(d)). The electron density is observed to flatten on a similar ($\sim 200\mu$sec) time scale. CHERS(Charge Exchange Recombination Spectroscopy) diagnostics also observe a flattening of the ion temperature after the crash although the time resolution of this diagnostic is as long as 50msec. The entire crash phase takes $150 - 800\mu$sec, while a sawtooth period is $100 - 200$ msec. The spatial ($<$ 6cm) and time ($\sim 10\mu$sec) resolutions of this representation were discussed with a description of the image reconstruction techniques in previous publications.[18–20]

To describe the electron heat flow pattern semi-quantitatively we approximate a time derivative of the electron temperature profile on a poloidal plane as

$$\delta T_e(r,\theta,t)/\delta t = [T_e(r,\theta,t+\tau) - T_e(r,\theta,t)]/\tau, \tag{1}$$

where, τ is the plasma's toroidal rotation period, typically 50μsec and usually much shorter than the crash phase period. Fig. 2 shows a typical heat flow pattern by overlaying a graded color representation for $\delta T_e(r,\theta,t)/\delta t$ on $T_e(r,\theta)$ contour lines for a sawtoothing discharge. The rotation period in this case is 120μsec. Blue shading represents a heat loss of approximately 1×10^4KeV/sec, and red a heat gain of 1×10^4KeV/sec. Frames a, b, c, and d of Fig. 2 refer to the same times as the corresponding frames in Fig. 1. During the period of development of the crescent-shaped flat temperature region, heat flow is essentially confined within the $q = 1$ radius. Fig. 2(b) shows heat flow around the circular high-temperature peak toward the intersection of the hot region with the $q = 1$ surface (X-region). Fig. 2(c),(d) shows transfer of heat through the X-region to the outside of the $q = 1$ radius. Later, we present a heuristic model in which partial magnetic reconnection causes anomolously fast heat flow through the X-region.

A more accurate presentation with a better time resolution of heat flow is shown in Fig. 3. Here, color contours of $\delta T_e(r,\theta,t)/\delta t$, together with $T_e(r,\theta)$ contours (solid lines), are shown for a discharge with a shorter rotation period of $\tau = 54\mu$sec. The four frames that make up Fig. 3 correspond to the time values (a)$t = 206\mu$sec, (b)$t = 314\mu$sec, (c)$t = 368\mu$sec, and (d)$t = 422\mu$sec. Here, $t = 0$ refers to the time at which an $m/n = 1/1$ precursor oscillation was first detected. Again, blue shading represents a heat loss of approximately 1×10^4Kev/sec, and red a heat gain of 1×10^4KeV/sec. During the period of development of the 1/1 mode, heat flow is essentially confined within the $q = 1$ radius. Fig. 3(a) and Fig. 3(b) show heat flow around the base of the circular high-temperature peak toward the intersection of the hot region with the $q = 1$ surface (X-region). Fig. 3(c),(d) show transfer of heat through the X-region to $r > r(q = 1)$, then away from the X-region. Fast 1-D radial electron heat transport outside of the $q = 1$ radius has been studied during and after the crash as a propagating heat pulse by Fredrickson et.al..[24]

III. Measurement of q-profile by Motional Stark Effect

We employ the motional Stark effect diagnostic to obtain the profile of magnetic pitch angle, and hence the q profile, using polarimetry measurements of the Doppler shifted D_α emission from a neutral deuterium–beam (NBI) heating line.[25,26,21] As a neutral beam penetrates through a plasma, collisions with background plasma ions

and electrons excite beam atoms, leading to D_α emission. By measuring the polarization of the "σ component" of the beam fluorescence, the pitch angle of the magnetic field lines can be determined wherever the beam penetrates the plasma. An important advantage of this technique is that the noninvasive and nonperturbative measurement of the field-line pitch is localized to the geometric intersection of the field of view with the neutral beamlines, which leads to good spatial resolution of $\delta r = 3 \sim 5$cm. The time resolution is as short as 5msec but typically 10msec.

If the plasma is considered to have good flux surfaces, the measured field line pitch can be translated into a radial profile of the safety factor, $q(R)$, based on tokamak equilibrium calculations. ECE and interferometer diagnostic measurements show that T_e and n_e profiles are axisymmetric throughout the sawtooth period except during the crash phase, suggesting that magnetic flux surfaces are also axisymmetric. The next section describes how the $q(R)$ profile may be derived from the measured pitch angle data.

IV. q-profile determination from pitch angle data

The relationship of magnetic field pitch angle to the $q(R)$ profile depends on the configuration (aspect ratio, a/R, elongation, triangularity) and on plasma parameters such as poloidal beta and internal plasma inductance.[27] For TFTR plasmas at modest beta, it is a good approximation to assume that magnetic flux surfaces form a nested set of shifted circles on a poloidal plane, i.e.,

$$X = R - \Delta(r) - r\cos\theta, \tag{2}$$

$$Z = r\sin\theta. \tag{3}$$

Here R is the magnetic axis location, $\Delta(r)$ is the Shafranov Shift (distance between magnetic axis and center of flux surfaces), and r is the minor radius of a flux surface.

Consider the conventional definition of magnetic field for an axisymmetric toroidal system:

$$\mathbf{B} = B_0 R_0 \Big[\nabla\phi \times \nabla\chi(r) + g(r)\nabla\phi\Big], \tag{4}$$

where, χ is the poloidal flux within a flux surface labelled by coordinate r, and g is the toroidal flux function. The shifted circle approximation allows a straightforward derivation of a closed-form expression for the safety factor $q(r)$. From the definition

$$q = \frac{1}{2\pi}\int_0^{2\pi} \frac{\mathbf{B}\cdot\nabla\phi}{\mathbf{B}\cdot\nabla\theta} d\theta, \tag{5}$$

we eliminate χ'/g in favor of the midplane magnetic pitch angle, γ, using

$$\tan\gamma_\pm \equiv B_p/B_t(X_\pm) \tag{6}$$

$$= \pm\frac{\chi'}{g(1\pm\Delta')}. \tag{7}$$

Here prime denotes derivative with respect to r, pitch angle is regarded as a function of midplane radius X, and $+/-$ refers to outboard/inboard with respect to the magnetic axis. The required θ integration yields

$$q(r) = \pm\frac{r}{R\tan\gamma_\pm(1\pm\Delta')}\left[-\frac{R\Delta'}{r}+\left(1+(R-\Delta)\frac{\Delta'}{r}\right)/\sqrt{(1-\frac{\Delta}{R})^2-(\frac{r}{R})^2}\right], \tag{8}$$

where

$$\tan\gamma_+(1+\Delta') = -\tan\gamma_-(1-\Delta') \tag{9}$$

is a constraint which follows from Eq. (7) and the fact that χ' and g are constant on a given flux surface.

MSE data provides pitch angle information for a range of midplane X values. Within the range, the pitch angle data may be fit to a continuous function: $\tan\gamma_\pm \equiv T_\pm \Rightarrow T(X)$. If the range spans the magnetic axis, the axis location $X = R$ is determined from the zero of $T(X)$. Consider now two possibilities:

(P1) The range of X for which pitch angle data is obtained spans a region roughly <u>centered</u> on the magnetic axis. In this case we can rewrite Eq. (9) as

$$\Delta' = \frac{T_+ + T_-}{T_+ - T_-}, \tag{10}$$

showing that $\Delta'(r)$ and hence $q(r)$ can be calculated from knowledge of pitch angle data on both sides of the magnetic axis. We note that Eq. (10) is nonlinear in Δ, since the arguments of $T_\pm$ are $X_\pm = r \mp \Delta(r)$. An effective solution procedure is to expand $\Delta(r)$ in a linear combination of radial basis functions and to solve Eq. (10) by a combination of iteration and least squares fitting.

Now consider the second possibility, which is relevant for the MSE set-up on TFTR:

(P2) Pitch angle data is obtained in a range of X values which includes the magnetic axis, but which lies predominantly between the magnetic axis and the outboard plasma edge. R is again determined by the zero of $T(X)$, however Eq. (9) can no

longer be used to determined Δ' since the right side of the equation is unknown for most of the window. The equation relating the data to the Shafranov Shift is now Eq. (7), i.e.,

$$\tan\gamma_+ = \frac{\chi'}{g(1+\Delta')}, \tag{11}$$

which is a single equation in (effectively) two unknowns; Δ' and the ratio χ'/g. An additional assumption is needed to determine the plasma geometry, and hence $q(r)$, from the pitch angle data.

To proceed, we assume that Δ' is determined by an inverse aspect ratio expansion of the plasma equilibrium equations. To leading order in the aspect ratio and assuming the standard low beta tokamak ordering,[27] we have $g = 1$ and Δ' related to χ' through

$$\Delta'(r) = \frac{1}{Rr\chi'^2}\int^r (\chi'^2 - 2rp'/B_0^2)rdr \tag{12}$$

$$= \frac{r}{R}(\tilde{\beta}_\theta + \tilde{\ell}_i/2) \tag{13}$$

where

$$\tilde{\beta}_\theta(r) = -\frac{1}{r^2\chi'^2}\int^r \frac{2r^2p'}{B_0^2}dr, \tag{14}$$

$$\tilde{\ell}_i/2(r) = \frac{1}{r^2\chi'^2}\int^r \chi'^2 rdr \tag{15}$$

are poloidal beta and internal inductance profile functions. For the simplest approximation, assume a constant current density and a parabolic pressure profile in the plasma. Then χ' and p' are linear in r and

$$\Delta(r) = \frac{r^2}{2R}(\beta_\theta + \ell_i/2) \tag{16}$$

where β_θ and ℓ_i are constant, and $\ell_i = 0.5$. For more general profiles, eg., $J(r) = J_0(1 - r^2/a^2)^{\alpha_J}$ and $p(r) = p_0(1 - r^2/a^2)^{\alpha_p}$ we can write

$$\Delta(r) = f(r;\alpha_p,\alpha_J)(\beta_\theta + \ell_i/2). \tag{17}$$

However, Eq. (16) has been shown to be accurate to within 5% for $\rho\beta_p/R_{\rm mag} < 0.5$ using the PEST[28] equilibrium code, and we use Eq. (8) and Eq. (16) for the present analysis. The combination $\beta_\theta + \ell_i/2$ is determined by magnetic measurements.

V. Measurement of q profiles

The q profiles before and after the sawtooth crash have been examined for typical neutral beam heated ($P_b = 8 - 11$MW) TFTR plasmas with toroidal current of $1.8MA$. Fig. 4 presents typical $q(R)$ profiles before and after a sawtooth crash. The statistical error in calculated q values is estimated to be less than 2.5%, although the systematic error is evaluated to be about 5% for $q(R)$ data based on a comparative analysis with the ECE inversion radii and by moving the magnetic axis radially for cross-calibration.[21] About two dozen similar discharges have been investigated and the central q values typically change between 0.70 and 0.80 during a sawtooth with a relative error of 2%. The central q values typically increase by 10% during the crash. This observation is in agreement with earlier results from TEXTOR and JET.[1]

Fig. 5(a) presents time evolution of central q values from MSE and the central electron temperature from the ECE signals in a typical sawtooth discharge. Correlated with the sawtooth collapse is a small rise of ~ 0.08 for q_0. In this example, as well as most TFTR discharges, q_0 is below one when sawteeth are present, and remains below unity throughout the sawtooth cycle. In order to reduce the statistical uncertainty and improve the time resolution, which is 30msec for the data shown here, we can synchronously or co-average the data over several sawteeth as shown in Fig. 5(b). Because only field-line breaking and re-arrangement can make a $q(R)$ change on such a short time scale ($\ll$ magnetic diffusion time), the observations verify a magnetic field-line reconnection, albeit small.

VI. Proposed Physical Model for Sawtooth Crash

The observations raise the question as to why the magnetic field lines inside the $q = 1$ region do not form a flat $q \sim 1$ inner region after the crash as suggested by Kadomtsev,[10] while the temperature gradient diminishes to zero as predicted by him for full reconnection. The clues to answering this question lie in the heat flow pattern shown in Fig. 2 and Fig. 3 during the crash phase.

The plasma may be viewed as concentric toroidal regions separated by the $q = 1$ surface. Plasma heating leads to an increase in pressure gradient, p', and a decrease in q_0. When p' exceeds a critical value depending on the local shear, an $m/n = 1/1$ ideal kink mode is triggered in the inner (core) region.[23] Flux surfaces are displaced rapidly outwards on an Alfven timescale (cf T_e profile in Fig. 1(b) and T_e contours in Fig. 2(b) and 3(a,b)). The plasma region outside of $q = 1$ plays the role of a stabilizing conducting shell which suppresses the flux displacements by inducing image currents near the interface of the core and shell. A current sheet and X-point are formed. Unlike the flux, the pressure is not so constrained by the outer region during the

kink evolution. In the last stage of development of the kink mode, the pressure and flux contours inside $q = 1$ do not coincide. The mismatch during this period is an important distinction from Kadomtsev's model which always assumes the pressure and flux surfaces coincide. We speculate that the observed enhanced perpendicular heat conduction is caused by a connection of different pressure contours by field lines of the mismatched flux surfaces. The local pressure gradient is strongest at the X-point (cf Fig. 2(b), 3(b) showing the steepest temperature gradient in the X-point region inside $q = 1$). The physics of finite resistivity in the current sheet now enters the problem, and reconnection takes place according to the standard reconnection theories.[3,4] A fast magnetic reconnection is induced at the X-point and a partial reconnection of magnetic field lines occurs connecting the crescent shaped inner region (see Fig. 1(b,c)) to the region outside of the inversion radius.[22,23] A rapid efflux of thermal energy occurs through the X-point region due to large parallel transport along newly connected field lines (cf Fig. 2(c,d) and 3(c,d)). Parallel plasma transport is so fast that the pressure equalization happens in a time much shorter than the theoretical magnetic reconnection time.[3,10] The time scale for this fast electron heat conduction process to equalize T_e on a poloidal contour is estimated to be the electron heat conduction time along field lines, $\pi R/v_e$ times $q/\Delta q$, where Δq denotes the width of q values in the reconnection region. This value, $\pi R/v_e q/\Delta q$ is about $10-20\mu$sec for $q/\Delta q \sim 10$ in the present plasma. The precipitous drop of the pressure gradient removes the free energy to drive the $m/n = 1/1$ instability, inhibiting further progress of the mode and thus full reconnection.

The drop in pressure gradient should induce a decrease in the central current density (increase in q_0) because of force balance. Such a change would lead to a decrease in the internal plasma inductance, ℓ_i. However, in a highly conducting plasma, flux conservation will inhibit a radical change of ℓ_i, and prevent complete flattening of the current and q profile inside $q = 1$. Consequently, the amount of the $q(R)$ change can be small, and q_0 does not have to rise to unity for $\nabla p \sim 0$. (Note that there are multiple solutions for $j(R)$ which satisfy $\mathbf{jxB} = \mathbf{0}$ for $q < 1$, if $\mathbf{j} \cdot \mathbf{B}/B^2$ is not constant[2] with respect to R).

VII. Discussion and Conclusions

A TRANSP analysis of the sawtoothing discharges provides a useful check on the amount of partial reconnection. The TRANSP[29] uses measured plasma profiles and the measured plasma boundary. Typically, measured profiles of the electron temperature (from ECE, Fig. 6(b)) and the temperature and toroidal rotation velocity of the trace carbon impurity (from neutral-beam induced charge-exchange recombination spectroscopy) are used as initial inputs. Profiles for the hydrogenic ion temperature

T_i are computed from the impurity ion temperature. Monte-Carlo techniques are used to compute the time evolution of the beam ions. The beam ions are assumed to slow down classically. The assumptions of classical slowing down and loss have been checked in the case of beam ions and DD fusion products. Approximately six seconds of the discharge evolution is modeled, starting about 0.5 sec after initiation and continuing through the neutral beam injection. For these experiments the neutral beam injection starts at 4 sec and extends to 6 sec.

Fig. 6 presents a set of plasma parameter evolutions (n_e, T_e) associated with sawtooth oscillations on which the TRANSP modeling are made, together with measured q_0 (by MSE), and $q_\psi(0)$ evolution deduced from the TRANSP calculation. The TRANSP plasma analysis code employs a phenomenological sawtooth model based on the helical flux mixing model.[10] which is invoked at the observed sawtooth crash times if $q_\psi(0) < 1$. The field lines are assumed to either not be mixed or to be only partly mixed by controling current density profile during the sawtooth crash and the results are compared with those from a case of the 100 % field-line mixing in the standard Kadomtsev model.[10] The TRANSP calculation can check whether the observed plasma profile evolutions are consistent with these current mixing models. Full field-line mixing predicts a $q_\psi(0)$ evolution between 0.9 and 1.0 and never reproduces the observed q_0 evolution to 0.70 - 0.85 during the crashes. On the other hand, 0% current-mixing (no reconnection) produces much lower $q_\psi(0)$ values than oberved, without any sawteeth. As shown in Fig. 6(d), a simulation based on a partial mixing of field lines (20-30%) leads to the best agreement with the experimental observations.

Evolution of central q values has been measured by several groups in the past few years.[12,13,17] There is agreement among all experiments that the relative change of central q during a sawtooth crash is small ($\Delta q/q \leq 0.1$). However, there is a major difference among the experiments on the final values of the central q after the crash. Wroblewski and Snider[17] recently reported that the central q values rise to 1 concluding that the observation is evidence of the Kadomtsev reconnection. Although the cause of this apparent disagreement with the present study is yet to be determined, it could be attributed to, 1) difficulties in $q(R)$ measurements and their analysis as noted by Wroblewski and Snyder,[17] and/or 2) DIII-D generates non circular plasmas[17] with different MHD properties from circular TFTR plasmas. We also note that most of the results that reported $\Delta q < 0.1$ during sawtooth crash can be explained by our proposed model.

In summary, magnetic reconnection consistent with partial mixing of field-lines during a sawtooth crash, and small changes of central q have been documented. The motional Stark effect(MSE) diagnostic has been employed to measure the pitch angle profile of magnetic field lines, and hence the q profile. An analytical relationship between the pitch angle of field lines and q profile has been developed for a toroidal

plasma with circular cross section. It has been shown that central q values stay substantially below 1, despite T_e contour evolution from ECE diagnostics which show full Kadomtsev-like 2-D reconnection patterns. A simultaneous analysis of poloidal $T_e(r,\theta)$ and $q(R)$ profile evolutions has led us to propose a heuristic model consistent in most of its features with that of Baty et al[23] which was based on a non-linear 3-D MHD numerical simulation. In our model an $m/n = 1/1$ ideal kink mode develops inside of the $q = 1$ radius and induces a partial rearrangement of field lines, i.e., partial reconnection, through the X-point region where a circular hot spot touches the $q = 1$ surface. A fast parallel transport along newly connected field lines can cause a rapid efflux of internal energy through the X-point region and therefore a fast crash of the central plasma pressure. The small change of q values associated with partial reconnection of field-lines is attributed to the precipitous drop of pressure gradients which drive the instability and the reconnection process, as well as a flux conservation principle.

VIII. Acknowledgements

Many valuable discussions with Drs. K. McGuire, W. Park, W. Stodiek, and L. Zakharov were highly appreciated. We also acknowledge skilled assistance by W. Davis and J. Stori. This work was supported by US. Department of Energy Contract No.DE-AC02-76-CHO3073.

Figures

FIG. 1. $T_e(r,\theta)$ profiles in 3-D during the crash period of sawtooth. Heat transfer ΔT_e is superposed with coded color contours. The time interval between each figure is $\sim 120\mu$sec.

FIG. 2. Heat flow (in color) superimposed on $T_e(r,\theta)$ contours (solid lines) for times corresponding to Fig.1(a-d). Blue represents a heat loss of about 1×10^4KeV/sec and red a gain of 1×10^4KeV/sec. The rotation period is 120μsec. The dashed line represents the inversion radius which is close to the $q = 1$ surface.

FIG. 3. Heat flow contours (in color) superposed on $T_e(r,\theta)$ contours (solid lines) for $t = 216\mu$sec (a), 314μsec (b), 368μsec (c) and 422μsec (d). Blue represents a heat loss of about 1 x 10^4 KeV/sec and red a gain of 1 x 10^4 KeV/sec. The rotation period τ is 54μsec. The dashed lines depict the inversion radius which is close to the $q = 1$ radius measured by MSE.

FIG. 4. $q(R)$ profiles derived from MSE before and after a sawtooth crash. The magnetic axis is 276 ± 3cm, both from ECE diagnostics and TRANSP analysis. The inversion radius of the ECE is about 301cm, which agrees with the $q = 1$ radius from MSE, within the spatial resolution of the diagnostics.

FIG. 5. (a) Time evolution of central safety factor q_0 for a typical NBI heated L mode plasma together with the ECE based T_e signal.
(b) Synchronously co-averaged data for one sawtooth period from 9 consecutive sawteeth . The averaging time perod is 5msec for each point. The crash occurs at $t = 0$.

FIG. 6. Time evolution of measured central plasma parameters: (a) $n_e(0)$ from microwave interferometer; (b) $T_e(0)$ from ECE; (c) $q(0)$ from MSE; (d) $q(0)$ from TRANSP calculation. A partial reconnection model with a current mixing rate of 20$\sim$ 30 % agrees well with the measurement.

References

[1] *World Survey of Activities in Controlled Fusion Research* (Nuclear Fusion special supplement 1991], (international Atomic Energy Agency, Vienna, 1991).

[2] J. B. Taylor, Rev. Mod. Phys., **28**, 243 (1986).

[3] E.N. Parker, "Cosmical Magnetic Fields"(Oxford:Claredon Press, 1979).

[4] V.M. Vasyliunas, Rev. Geophys. Space. Phys., **13**, 303 (1975).

[5] R. L. Stenzel and W. Gekelman, J. Geophys. Res., **86**, 649 (1981).

[6] W. Gekelman and H. Pfister, Phys. Fluids, **31**, 2017 (1988).

[7] M. Yamada, Y. Ono, A. Hayakawa, M. Katsurai, and F.w. Perkins, Phys. Rev. Lett., **65**, 721 (1990). Y. Ono, A. Morita, M. Katsurai and M. Yamada Phys. Fluids **5**, 3691 (1993)

[8] S. von Goeler, W.Stodiek, and N.R. Sauthoff, Phys.Rev.Letts., **33**,1201(1974).

[9] J. A. Wesson, Tokamaks (Clarendon, Oxford, 1987), pp. 176-183.

[10] B. B. Kadomtsev, Sov., J. Plasma Phys., **1** , 389 (1975).

[11] J. A. Wesson, Plasma Phys. Contr. Fusion, **28**, 243 (1986).

[12] H. Soltwisch, Rev. Sci. Instrum., **59**, 1599 (1988).

[13] W.P. West, D.M. Thomas, J.S. DeGrassie, and S.M. Zhang, Phys. Rev. Lett., **58**, 2758 (1987).

[14] H. Weisen, G. Borg, B. Joye, A.J. Knight, and J.B. Lister, Phys. Rev. Lett., **62**, 434 (1989).

[15] R.C. Wolf, Nucl. Fusion **33**, 663 (1993).

[16] T.H.Osborne, R.N. Dexter, and S.C. Prager, Phys. Rev. Lett., **49**, 734 (1982).

[17] D. Wroblewski and R. Snider, Phys. Rev. Lett., **71**, 859 (1993).

[18] Y. Nagayama, R. Buchse, A. Cavallo, E.D. Fredrickson,A.c. Janos, K.M. McGuire, G.Kuo Petravic, C. Sule and G. Taylor, Rev. Sci. Instrum., **61**, 3265 (1990).

[19]Y. Nagayama, K.M. McGuire,M. Bitter, A. Cavallo, E.D. Fredrickson, K.W. Hill, H. Hsuan, A. Janos, W. Park, G. Taylor,and M. Yamada, Phys. Rev. Letts., **67**, 3527 (1991).

[20]M. Yamada, Y. Nagayama, W. Davis, E. Fredrickson, A. Janos, and F. Levinton, Rev. Sci. Instrum., **63**, 4623, (1992).

[21]F. M. Levinton, S.H. Batha, M. Yamada, and M.C. Zarnstorff, Phys. Fluids, **B5**, 2554 (1993).

[22]A.J. Lichtenberg, Nucl. Fusion **24**, 1277 (1984).

[23]H. Baty, J.F. Luciani, M.N. Bussac, Phys. Fluids **B5**, 1213, (1993).

[24]E. Fredrickson, Phys. Rev. Lett., **65**, 2869 (1990).

[25]F.M. Levinton, Rev. Sci. Instrum., **63**, 5157, (1992).

[26]F.M. Levinton, R.J. Fonck, G.M. Gammel,R. Kaita, H.W. Kugel, E.T.Powell, D.W. Roberts, Phys. Rev. Letts., **63**, 2060 (1989).

[27]J. M. Greene, J.L. Johnson,E. Weimer, Phys. Fluids **14**, 671 (1971).

[28]R.C. Grimm, J.M. Greene, and J.L. Johnson, Methods in Computational Physics, **16**, 253 (1976).

[29]R.V. Budny, M.G. Bell, H. Biglari, M. Bitter, C.E. Bush, C.Z. Cheng, E.D. Fredrickson, B. Grek, K.W. Hill, H. Hsuan, A.C. Janos, D.L. Jassby, D.W. Johnson,L.C. Johnson, B. Leblank, D.C. McCune. D. R. Mikkelson, H.K. Park, A.T. Ramsey, S.A. Sabbagh, S.D. Scott, J.F. Schivell, J.D. Strachan, B.C. Stratton, E.J. Synakowski, G. Taylor, M.C. Zarnstorff, and S.J. Zweben, Nuclear Fusion **32**, 429 (1992)

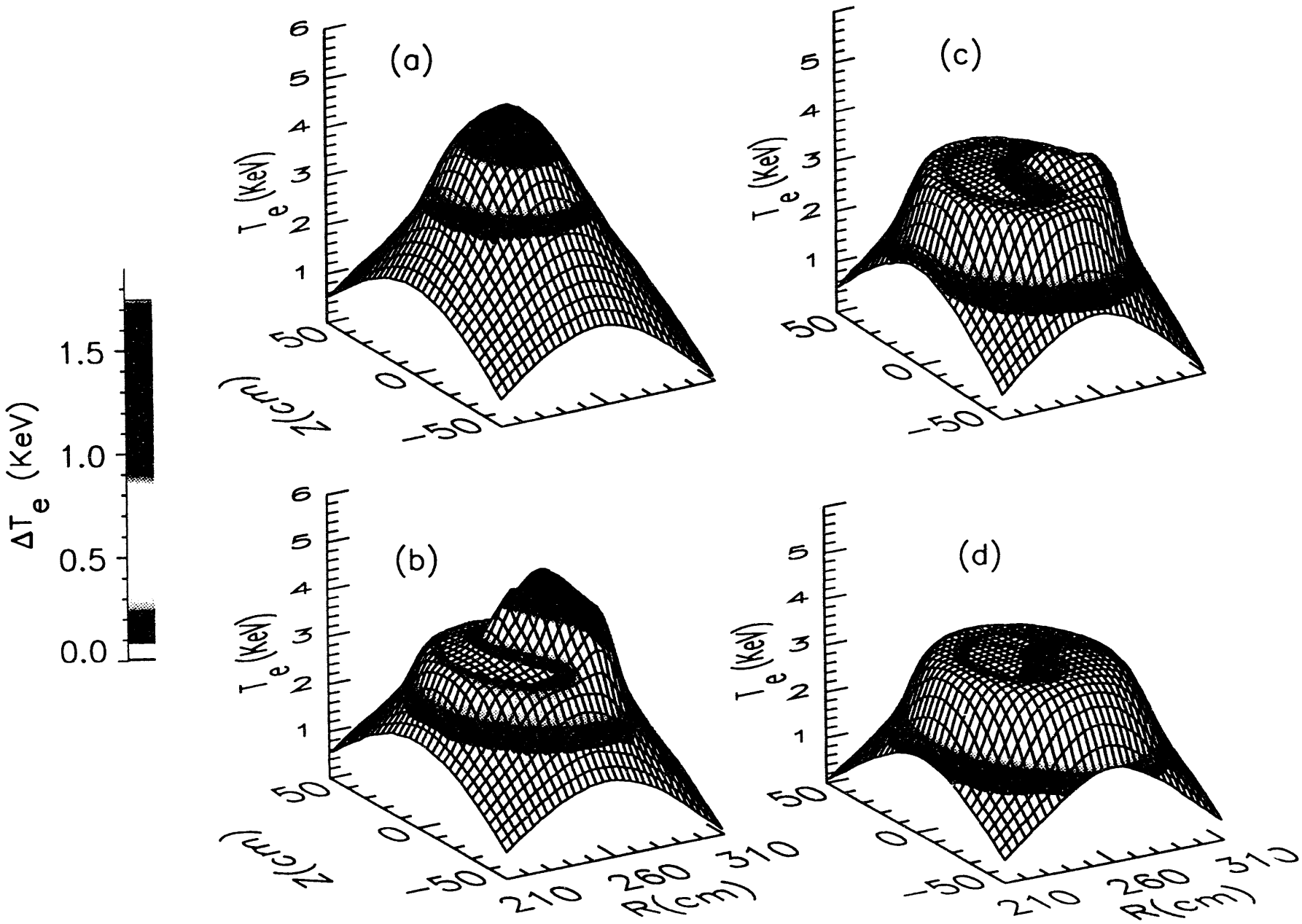

Fig. 1

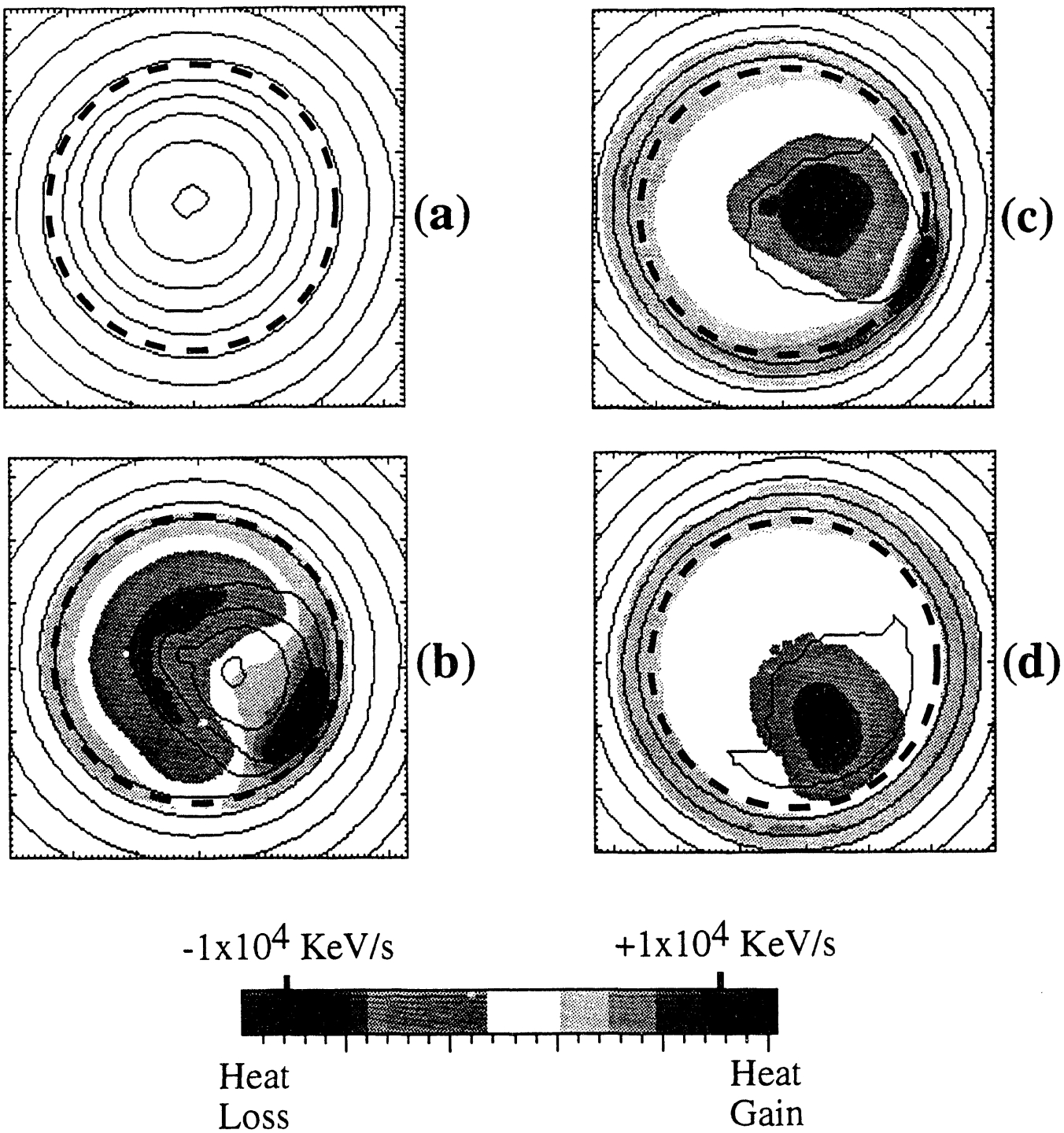

Fig. 2

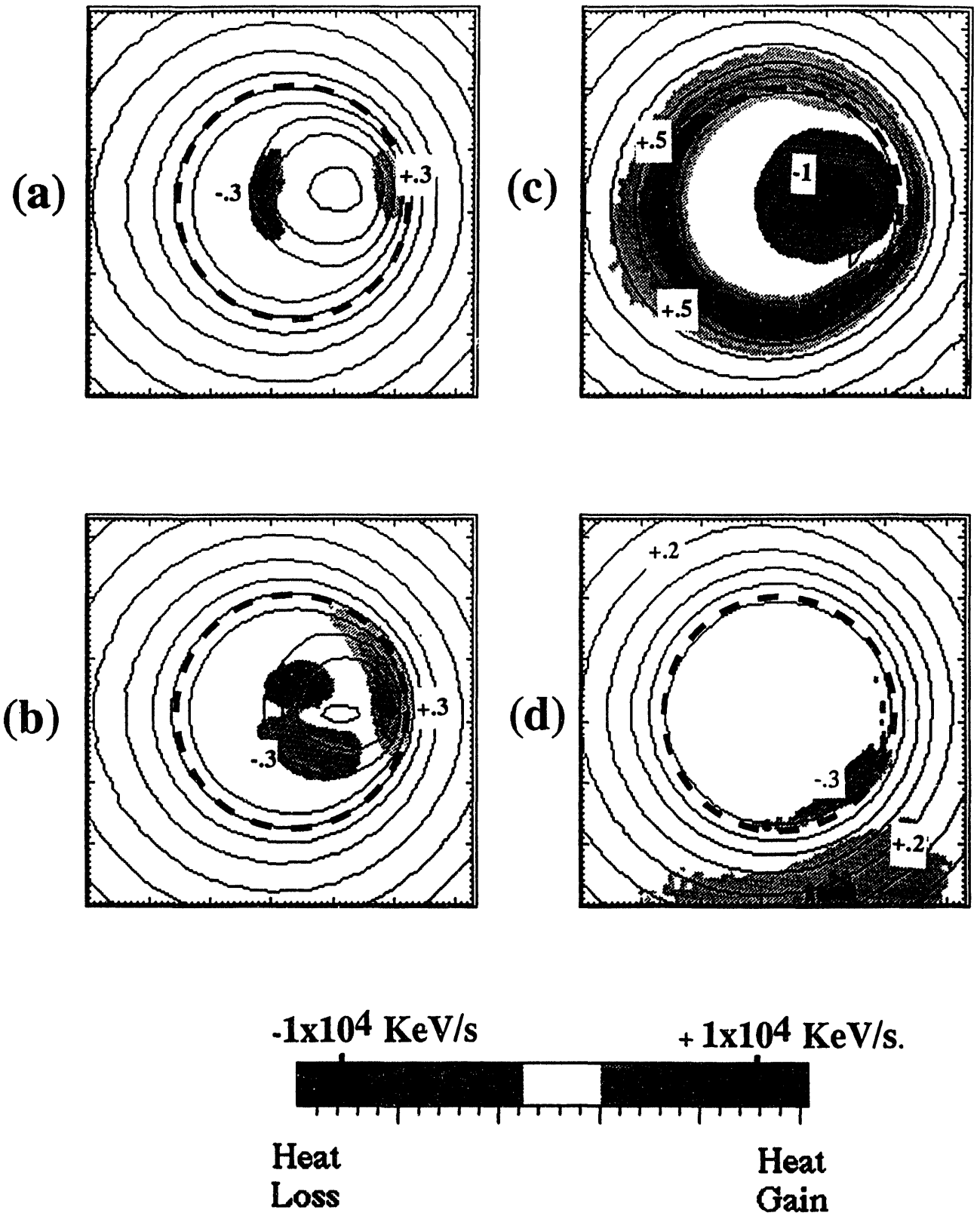

Fig. 3

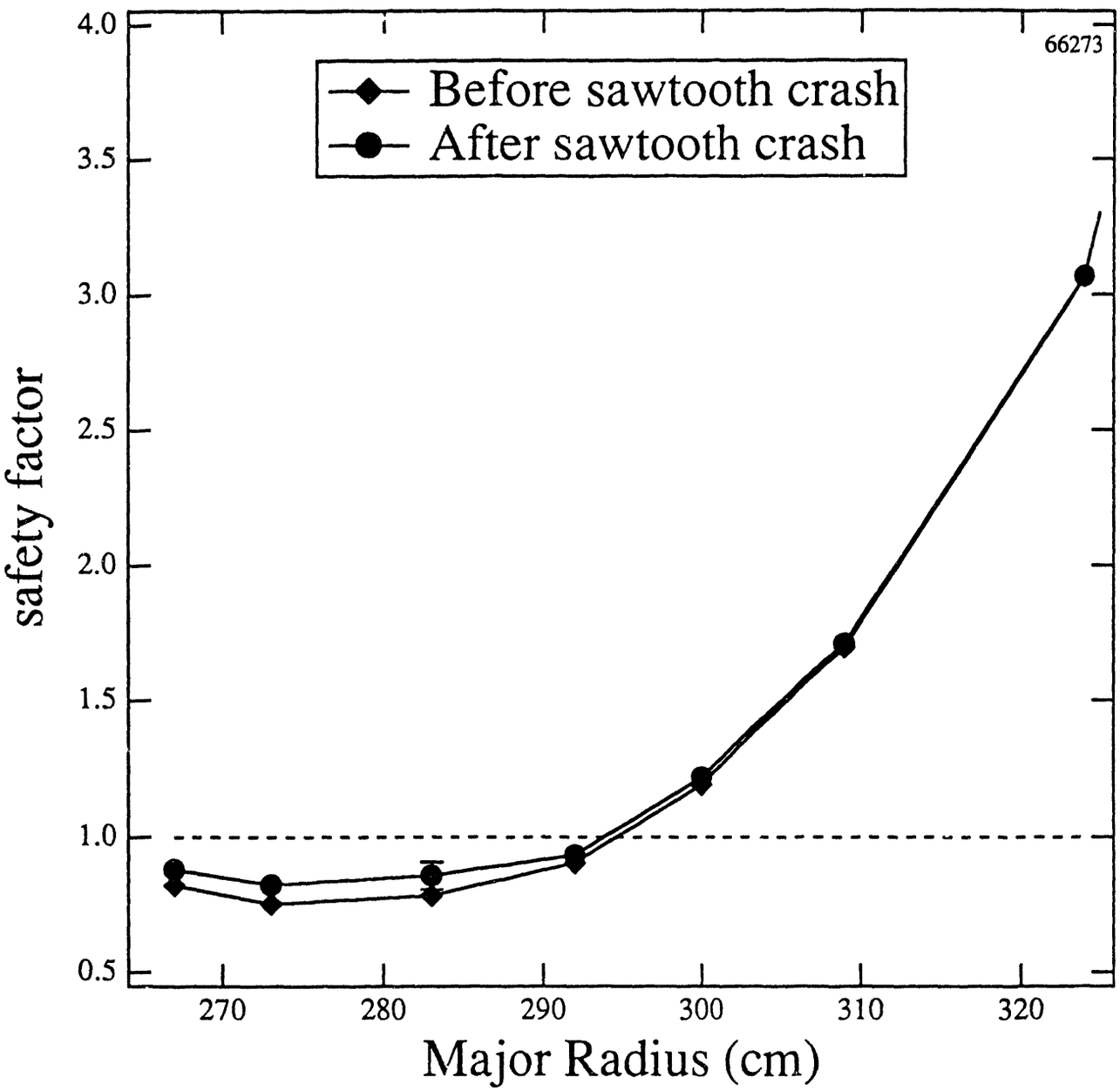
66273
Before sawtooth crash
After sawtooth crash
safety factor
4.0
3.5
3.0
2.5
2.0
1.5
1.0
0.5
270
280
290
300
310
320
Major Radius (cm)

Fig. 4

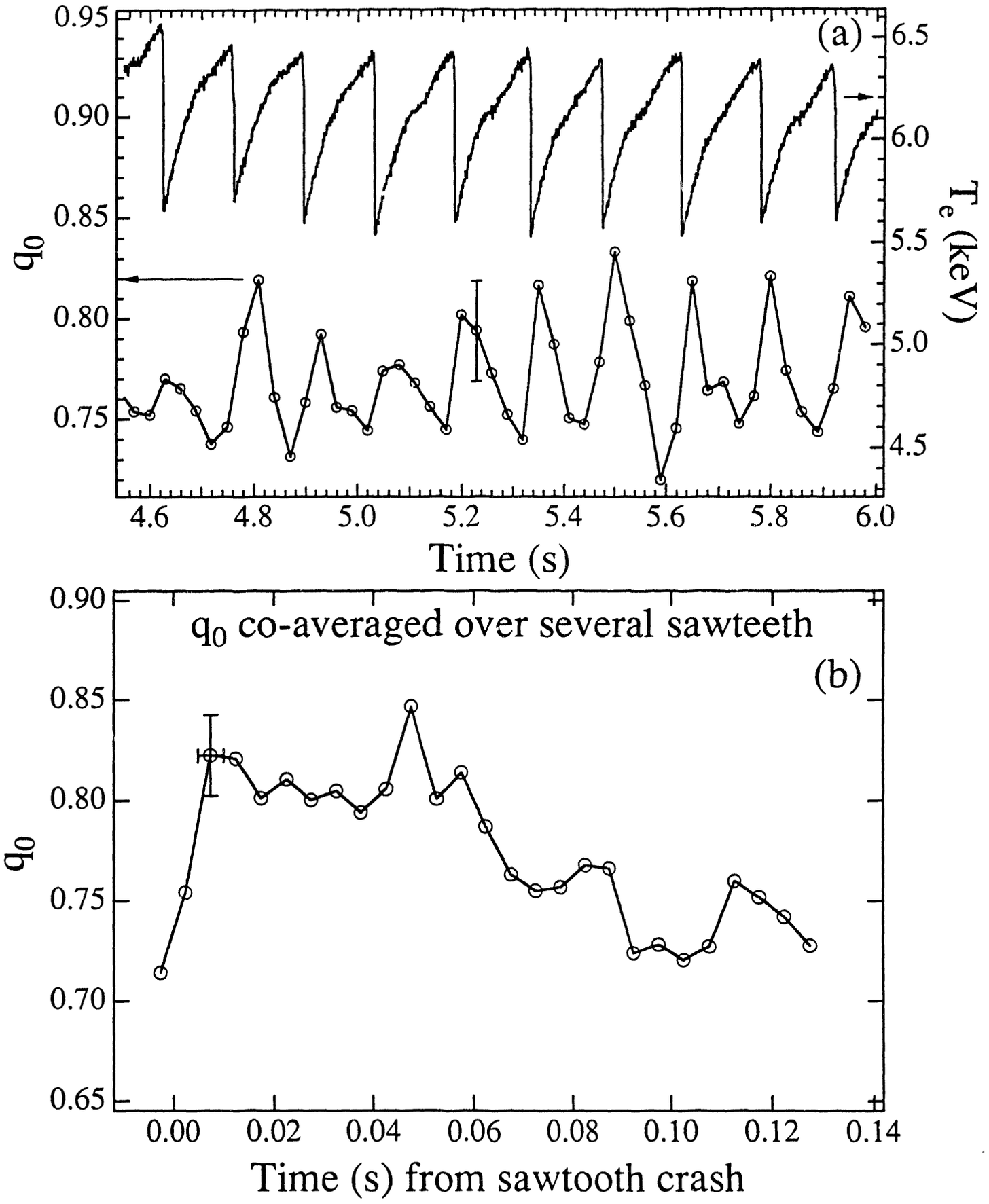
(a)
0.95
0.90
0.85
0.80
0.75
q_0
6.5
6.0
5.5
5.0
4.5
T_e (keV)
4.6
4.8
5.0
5.2
5.4
5.6
5.8
6.0
Time (s)
q_0 co-averaged over several sawteeth
(b)
0.90
0.85
0.80
0.75
0.70
0.65
q_0
0.00
0.02
0.04
0.06
0.08
0.10
0.12
0.14
Time (s) from sawtooth crash

Fig. 5

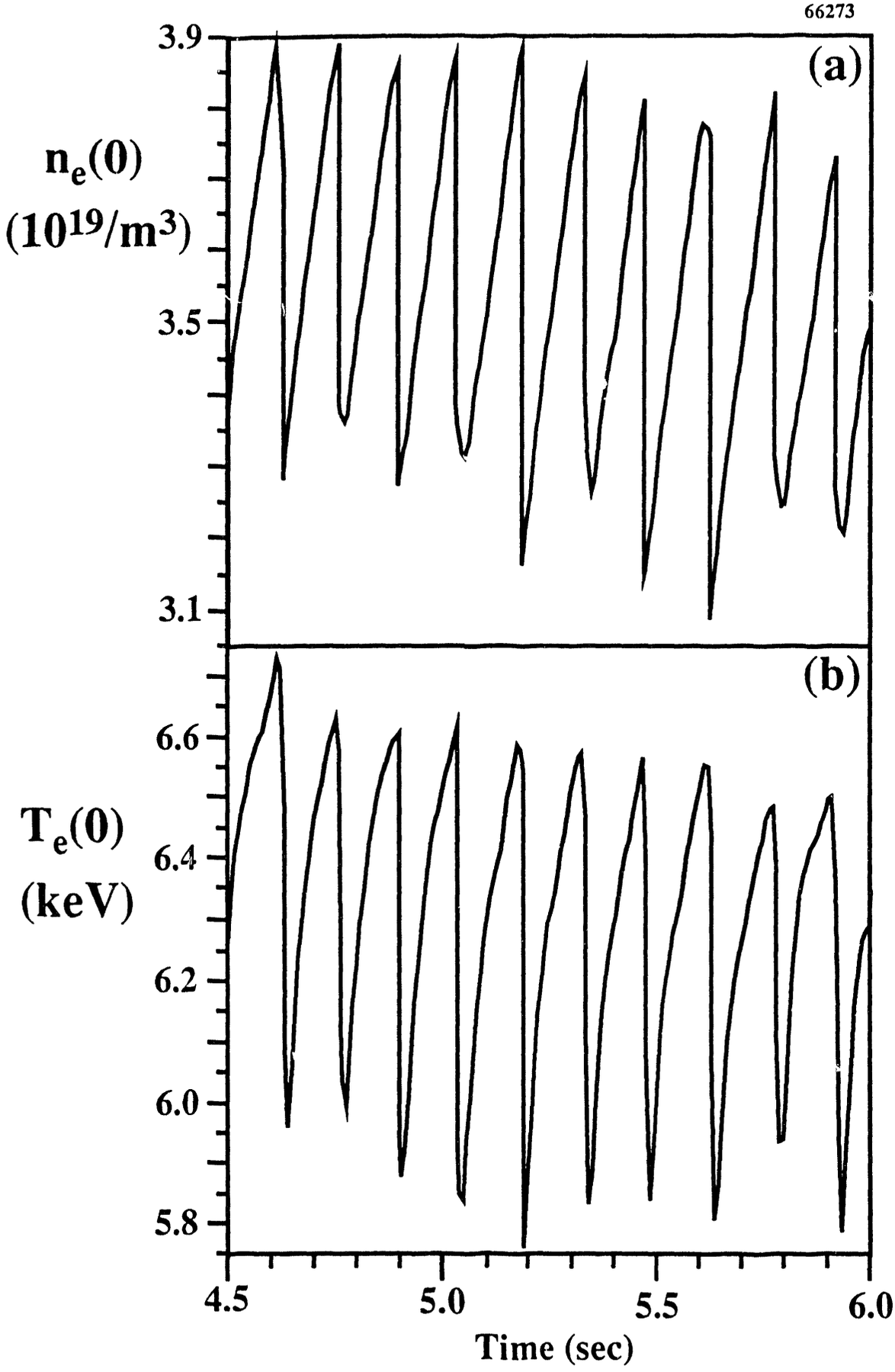
66273
(a)
(b)
$n_e(0)$
$(10^{19}/m^3)$
3.9
3.5
3.1
$T_e(0)$
(keV)
6.6
6.4
6.2
6.0
5.8
4.5
5.0
5.5
6.0
Time (sec)

Fig 6 (a,b)

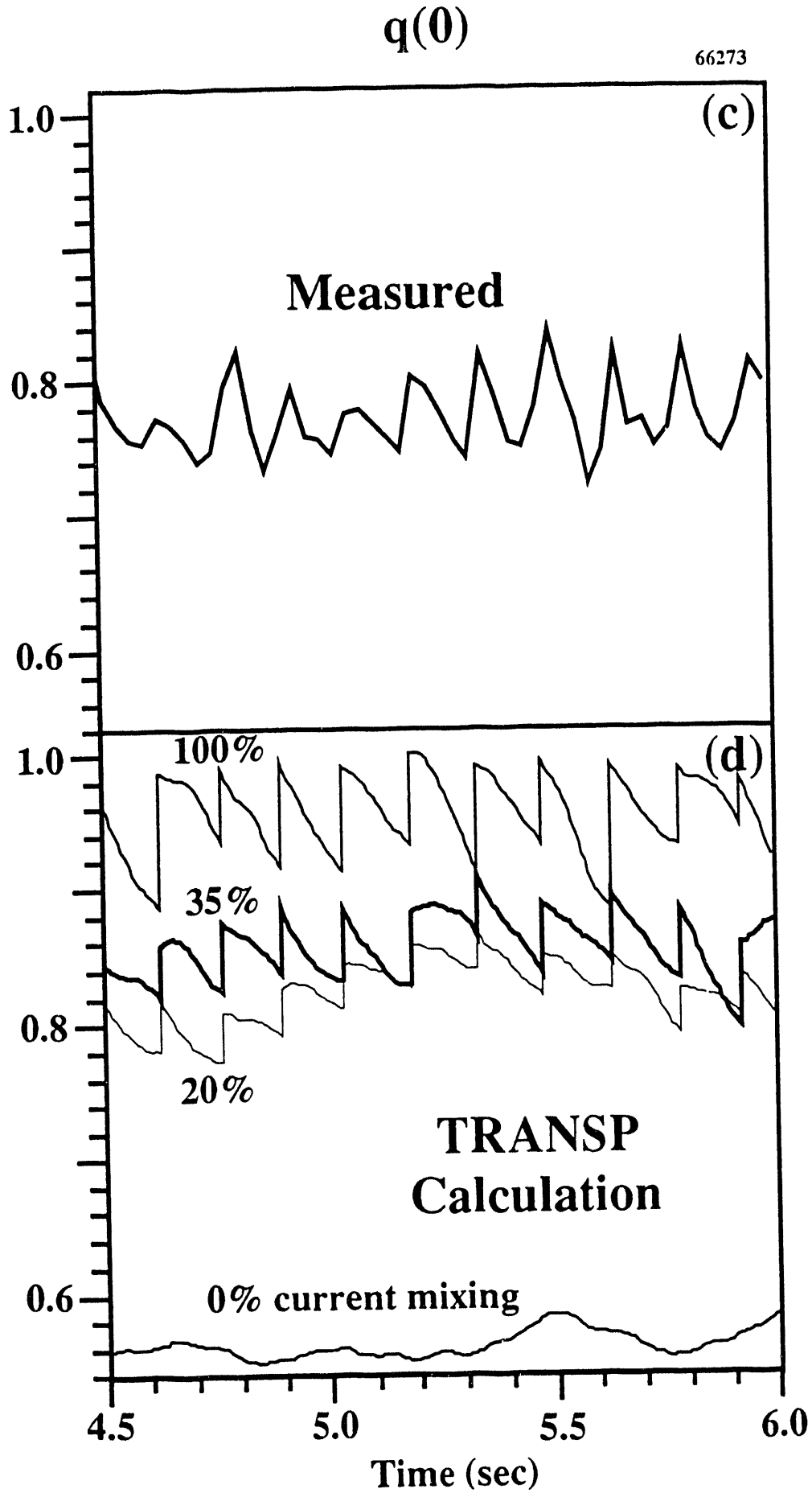
q(0)
66273
(c)
Measured
1.0
0.8
0.6
(d)
100%
35%
20%
TRANSP
Calculation
0% current mixing
1.0
0.8
0.6
4.5
5.0
5.5
6.0
Time (sec)

Fig. 6 (c,d)

EXTERNAL DISTRIBUTION IN ADDITION TO UC-420

Dr. F. Paoloni, Univ. of Wollongong, AUSTRALIA
Prof. R.C. Cross, Univ. of Sydney, AUSTRALIA
Plasma Research Lab., Australian Nat. Univ., AUSTRALIA
Prof. I.R. Jones, Flinders Univ, AUSTRALIA
Prof. F. Cap, Inst. for Theoretical Physics, AUSTRIA
Prof. M. Heindler, Institut für Theoretische Physik, AUSTRIA
Prof. M. Goossens, Astronomisch Instituut, BELGIUM
Ecole Royale Militaire, Lab. de Phy. Plasmas, BELGIUM
Commission-European, DG. XII-Fusion Prog., BELGIUM
Prof. R. Bouciqué, Rijksuniversiteit Gent, BELGIUM
Dr. P.H. Sakanaka, Instituto Fisica, BRAZIL
Prof. Dr. I.C. Nascimento, Instituto Fisica, Sao Paulo, BRAZIL
Instituto Nacional De Pesquisas Espaciais-INPE, BRAZIL
Documents Office, Atomic Energy of Canada Ltd., CANADA
Ms. M. Morin, CCFM/Tokamak de Varennes, CANADA
Dr. M.P. Bachynski, MPB Technologies, Inc., CANADA
Dr. H.M. Skarsgard, Univ. of Saskatchewan, CANADA
Prof. J. Teichmann, Univ. of Montreal, CANADA
Prof. S.R. Sreenivasan, Univ. of Calgary, CANADA
Prof. T.W. Johnston, INRS-Energie, CANADA
Dr. R. Bolton, Centre canadien de fusion magnétique, CANADA
Dr. C.R. James,, Univ. of Alberta, CANADA
Dr. P. Lukác, Komenského Universzita, CZECHO-SLOVAKIA
The Librarian, Culham Laboratory, ENGLAND
Library, R61, Rutherford Appleton Laboratory, ENGLAND
Mrs. S.A. Hutchinson, JET Library, ENGLAND
Dr. S.C. Sharma, Univ. of South Pacific, FIJI ISLANDS
P. Mähönen, Univ. of Helsinki, FINLAND
Prof. M.N. Bussac, Ecole Polytechnique,, FRANCE
C. Mouttet, Lab. de Physique des Milieux Ionisés, FRANCE
J. Radet, CEN/CADARACHE - Bat 506, FRANCE
Prof. E. Economou, Univ. of Crete, GREECE
Ms. C. Rinni, Univ. of Ioannina, GREECE
Preprint Library, Hungarian Academy of Sci., HUNGARY
Dr. B. DasGupta, Saha Inst. of Nuclear Physics, INDIA
Dr. P. Kaw, Inst. for Plasma Research, INDIA
Dr. P. Rosenau, Israel Inst. of Technology, ISRAEL
Librarian, International Center for Theo Physics, ITALY
Miss C. De Palo, Associazione EURATOM-ENEA , ITALY
Dr. G. Grosso, Istituto di Fisica del Plasma, ITALY
Prof. G. Rostangni, Istituto Gas Ionizzati Del Cnr, ITALY
Dr. H. Yamato, Toshiba Res & Devel Center, JAPAN
Prof. I. Kawakami, Hiroshima Univ., JAPAN
Prof. K. Nishikawa, Hiroshima Univ., JAPAN
Librarian, Naka Fusion Research Establishment, JAERI, JAPAN
Director, Japan Atomic Energy Research Inst., JAPAN
Prof. S. Itoh, Kyushu Univ., JAPAN
Research Info. Ctr., National Instit. for Fusion Science, JAPAN
Prof. S. Tanaka, Kyoto Univ., JAPAN
Library, Kyoto Univ., JAPAN
Prof. N. Inoue, Univ. of Tokyo, JAPAN
Secretary, Plasma Section, Electrotechnical Lab., JAPAN
Dr. O. Mitarai, Kumamoto Inst. of Technology, JAPAN
Dr. G.S. Lee, Korea Basic Sci. Ctr., KOREA
J. Hyeon-Sook, Korea Atomic Energy Research Inst., KOREA
D.I. Choi, The Korea Adv. Inst. of Sci. & Tech., KOREA
Prof. B.S. Liley, Univ. of Waikato, NEW ZEALAND
Inst of Physics, Chinese Acad Sci PEOPLE'S REP. OF CHINA
Library, Inst. of Plasma Physics, PEOPLE'S REP. OF CHINA
Tsinghua Univ. Library, PEOPLE'S REPUBLIC OF CHINA
Z. Li, S.W. Inst Physics, PEOPLE'S REPUBLIC OF CHINA
Prof. J.A.C. Cabral, Instituto Superior Tecnico, PORTUGAL
Prof. M.A. Hellberg, Univ. of Natal, S. AFRICA
Prof. D.E. Kim, Pohang Inst. of Sci. & Tech., SO. KOREA
Prof. C.I.E.M.A.T, Fusion Division Library, SPAIN
Dr. L. Stenflo, Univ. of UMEA, SWEDEN
Library, Royal Inst. of Technology, SWEDEN
Prof. H. Wilhelmson, Chalmers Univ. of Tech., SWEDEN
Centre Phys. Des Plasmas, Ecole Polytech, SWITZERLAND
Bibliotheek, Inst. Voor Plasma-Fysica, THE NETHERLANDS
Asst. Prof. Dr. S. Cakir, Middle East Tech. Univ., TURKEY
Dr. V.A. Glukhikh,Sci. Res. Inst. Electrophys.I Apparatus, USSR
Dr. D.D. Ryutov, Siberian Branch of Academy of Sci., USSR
Dr. G.A. Eliseev, I.V. Kurchatov Inst., USSR
Librarian, The Ukr.SSR Academy of Sciences, USSR
Dr. L.M. Kovrizhnykh, Inst. of General Physics, USSR
Kernforschungsanlage GmbH, Zentralbibliothek, W. GERMANY
Bibliothek, Inst. Für Plasmaforschung, W. GERMANY
Prof. K. Schindler, Ruhr-Universität Bochum, W. GERMANY
Dr. F. Wagner, (ASDEX), Max-Planck-Institut, W. GERMANY
Librarian, Max-Planck-Institut, W. GERMANY

DATE
FILMED
10/21/94

END